applied sciences

MDPI

Article

# Modelling the Uptake of $^{226}$Ra and $^{238}$U Stable Elements in Plants during Summer in the Vicinity of Tailings from an Abandoned Copper Mine

**Víctor Manuel Expósito-Suárez [1,2], José Antonio Suárez-Navarro [1,*], Miguel Morales-Quijano [2], María Belén Gómez-Mancebo [1], Marta Barragan [1], Miriam Cortecero [3] and José Francisco Benavente [1]**

[1] Centro de Investigaciones Energéticas, Medioambientales y Tecnológicas (CIEMAT), Avenida Complutense 40, 28040 Madrid, Spain; victormanuel.exposito@ciemat.es (V.M.E.-S.); mariabelen.gomez@ciemat.es (M.B.G.-M.); marta.barragan@ciemat.es (M.B.); jf.benavente@ciemat.es (J.F.B.)
[2] Facultad de Ciencias Químicas, Universidad Complutense de Madrid, Plaza de las Ciencias, 2, Moncloa–Aravaca, 28040 Madrid, Spain; mimora01@ucm.es
[3] IES Virgen de la Paloma, C/de Francos Rodríguez, 106, 28039 Madrid, Spain; miriamcortecero63@gmail.com
* Correspondence: ja.suarez@ciemat.es

check for updates

**Citation:** Expósito-Suárez, V.M.; Suárez-Navarro, J.A.; Morales-Quijano, M.; Gómez-Mancebo, M.B.; Barragan, M.; Cortecero, M.; Benavente, J.F. Modelling the Uptake of $^{226}$Ra and $^{238}$U Stable Elements in Plants during Summer in the Vicinity of Tailings from an Abandoned Copper Mine. *Appl. Sci.* **2024**, *14*, 9201. https://doi.org/10.3390/app14209201

Academic Editor: Apostolos Giannis

Received: 23 August 2024
Revised: 30 September 2024
Accepted: 7 October 2024
Published: 10 October 2024

**Abstract:** Transfer factors (TFs) are widely used tools for assessing the uptake of radionuclides by plants. The literature contains numerous studies on TFs in tropical and temperate climates; however, the existing data on TFs in arid and semi-arid climates are very scarce. Furthermore, the current trend in nuclear energy expansion in countries with this type of climate necessitates knowledge of the mechanisms of radionuclide incorporation by plants as well as the TF values. For this reason, this work investigates the TFs of $^{238}$U and $^{226}$Ra in plants in a study area during the summer period under conditions equivalent to a semi-arid climate. The selected plants were *Scolymus hispanicus* L., *Eryngium campestre* L., *Chenopodium vulvaria* L., and *Chenopodium album* L., which were collected in the vicinity of a waste dump from an abandoned copper mine. The selected study area has radionuclide levels above the global average, in addition to heavy metals, as it is a waste dump from an abandoned copper mine. The range of transfer factors for $^{238}$U varied between $1.5 \times 10^{-4}$ kg$^{-1}$ kg$^{-1}$ and $7.8 \times 10^{-3}$ kg$^{-1}$ kg$^{-1}$, while for $^{226}$Ra, the range was between $1.8 \times 10^{-4}$ kg$^{-1}$ kg$^{-1}$ and $4.0 \times 10^{-2}$ kg$^{-1}$ kg$^{-1}$. The correlations found with PCA were (i) $^{238}$U with Fe and Al, and (ii) $^{226}$Ra with S, Ti, Ca, and Sr. A transfer model of $^{238}$U and $^{226}$Ra was created using multiple linear regression analysis. The model showed how $^{238}$U was related to the presence of Al, while $^{226}$Ra was related to Al, Fe, and Ti. The results obtained have allowed us to propose a model for the incorporation of $^{238}$U and $^{226}$Ra, taking into account the chemical composition of the soil. The results obtained indicate that both *Scolymus hispanicus* L. and *Eryngium campestre* L. could be utilized in phytoremediation for soils contaminated by natural radionuclides in semi-arid climates. The TFs, as well as the proposed model, allow us to expand the knowledge of the absorption of natural radionuclides by plants in regions with arid and semi-arid climates, which is necessary for the radiological risk assessment of future nuclear fuel cycle facilities.

**Keywords:** transfer factors; uranium; radium; natural radioactivity

## 1. Introduction

The uptake of radionuclides such as $^{238}$U and $^{226}$Ra by plants is a well-studied aspect of the literature [1–5]. The parameter used to evaluate the availability and uptake of radionuclides by plants is the transfer factor [6]. This parameter is defined as the dry mass ratio of the activity concentration of a given radionuclide in a plant to its content in the soil. The values reported in the literature for $^{238}$U and $^{226}$Ra range widely from $10^{-4}$ to 1 kg$^{-1}$ kg$^{-1}$ [6–8]. The high variability in transfer factors is mainly because they are a very conservative parameter, as they do not take into account the interactions of radionuclides with the physicochemical properties of soil [9,10]. In relation to this, there are few studies that relate chemical composition regarding the concentration of stable elements with unstable or radioactive ones such as $^{226}$Ra and $^{238}$U [11]. Rea et al. [12] studied the uptake of radionuclides from the uranium and thorium radioactive series considering the presence of stable elements; however, the study did not relate the uptake of stable elements with the natural radionuclides. Similarly, Vera-Tomé et al. [13] found no correlation between the stable elements and the natural radionuclides. Therefore, more studies are needed on this possible relationship in the uptake of stable and radioactive elements by plants.

On the other hand, the study of the uptake of both naturally occurring and artificial radionuclides by plants in semi-arid climates is increasing in importance due to the absence of transfer factors for these types of climates [14]. The soils typical of these climates possess characteristics that distinguish them those of from tropical climates and affect plant absorption. The primary characteristic is a lack of moisture, mainly due to the texture and absence of organic matter, which results in high-level water stress for the plants [14,15]. Additionally, temperatures cause precipitation to evaporate quickly, leading to radionuclides being retained in the surface layer of the soils, making them less accessible to the roots [1]. These characteristics imply that fewer radionuclides are incorporated than those in the soils of tropical climates, which have a greater presence of organic matter and moisture. The need for this knowledge lies in the possible future construction of nuclear power plants in countries with this type of climate in the near future. The literature includes many studies of this type of climate for different radionuclides, both naturally occurring and anthropogenic, and for different types of soils, including in areas impacted and not impacted by uranium mining [1,16–19]. However, these studies only report transfer factors, without finding a relationships between the studied radionuclides and the stable elements. The transfer factors are used to assess the potential incorporation of radionuclides through the food chain. The initial step involves the ingestion of plants by livestock, which may subsequently be consumed by humans, potentially increasing the risk of cancer [20].

The objective of this study was to investigate the potential relationship between the uptake of two major natural radionuclides, $^{238}$U and $^{226}$Ra, by plants and stable elements in a semi-arid climate. The necessary conditions for this study were provided by the waste heap and the surroundings of an abandoned Cu mine during the summer period, where the absence of rainfall and high temperatures resembled a semi-arid climate zone. Our working hypothesis was that there is a relationship between the uptake of $^{238}$U and $^{226}$Ra and stable elements under semi-arid climate conditions. To test our hypothesis, the partial objectives were (i) the radiological and chemical characterization of the soils in the study area, (ii) the determination of the transfer factors of $^{238}$U and $^{226}$Ra, along with those of the stable elements in four types of plants (*Scolymus hispanicus* L., *Eryngium campestre* L., *Chenopodium vulvaria* L., and *Chenopodium album* L.), and (iii) the statistically relation of the transfer factors through principal component analysis, obtaining absorption models through multiple linear regression analysis.

## 2. Materials and Methods

### *2.1. Study Area and Plants Analyzed*

The waste heap of the "Antigua Pilar" mine is located in the municipality of Colmenarejo in the western part of the Community of Madrid (Spain) (Figure 1). The area is situated at an elevation between 780 and 815 m, with an average temperature of 13.4 °C and an annual precipitation average of 637 mm. The soils in the Colmenarejo area are classified as cambisols formed from granites, gneisses, mica schists, and quartz [21]. Summer temperatures can reach up to 35 °C, which combined with the absence of precipitation, gives the climate a semi-arid character.

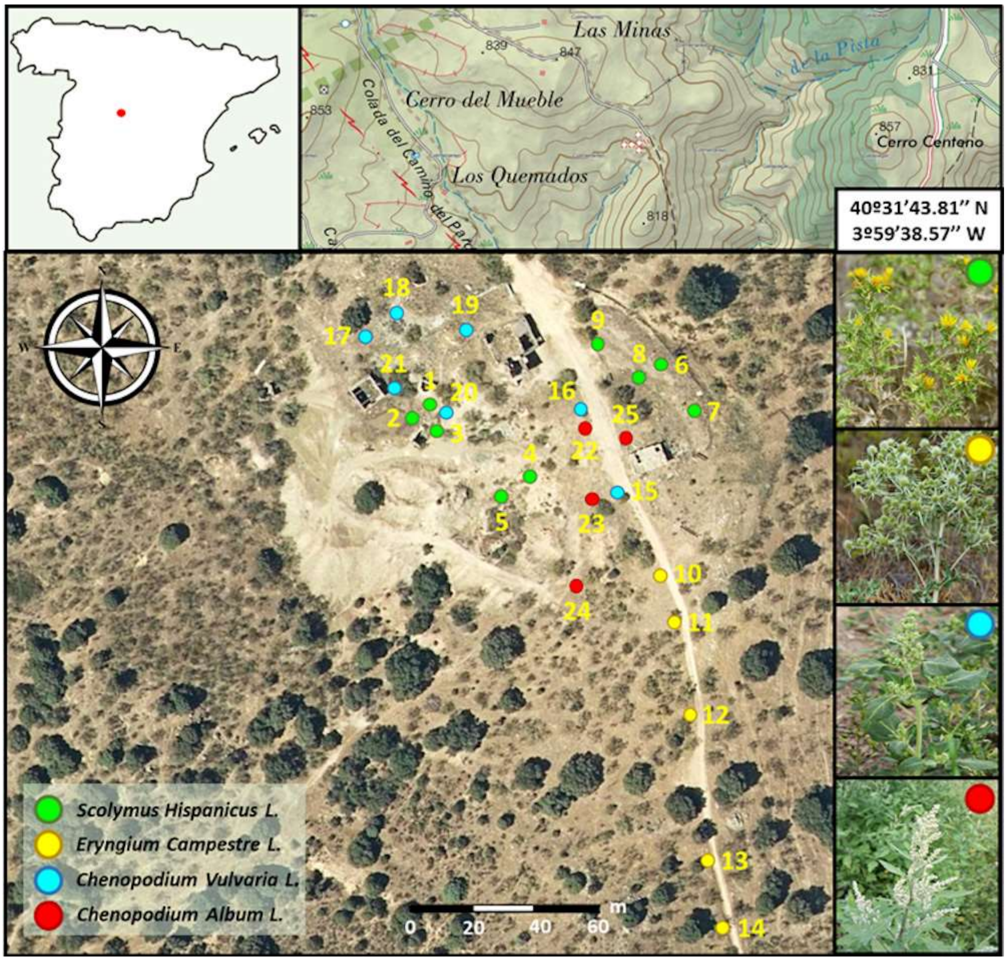

**Figure 1.** The location of the sampling points of the 25 plants collected from the surroundings and in the tailings of the Antigua Pilar copper mine.

The study area was the abandoned waste heap of the "Antigua Pilar" copper mine in the municipality of Colmenarejo in the Community of Madrid (Spain). The mine's waste heap mainly contains the following minerals: chalcopyrite ($CuFeS_2$), arsenopyrite ($FeAsS$), malachite ($Cu_2CO_3(OH)_2$), azurite ($Cu_3(CO_3)_2(OH)_2$), pyrite ($FeS_2$), siderite ($FeCO_3$), fluorite ($CaF_2$), olivenite ($Cu_2AsO_4(OH)$), and chalcanthite ($CuSO_4\cdot 5H_2O$) [C1196]. In addition to these minerals, the mine's waste heap contains torbernite ($Cu(UO_2)_2(PO_4)_2\cdot 8$–$12H_2O$) and zeunerite ($Cu(UO_2)_2(AsO_4)2\cdot 12H_2O$), whose presence is caused by geological formation through hydrothermal processes [22]. Therefore, the samples from the waste heap and its surroundings have a ratio of the activity concentration of uranium and thorium radioactive series that is significantly greater than 1 [23]. Figure 2a–c depicts the mine tailings pile and a detailed view of the minerals present. The four plant species used in this study were selected based on their relevance to the following aspects: (i) *Scolymus hispanicus* L. (9 plants) for its use in phytoremediation by absorbing numerous heavy metals [24]; (ii) *Eryngium campestre* L. (5 plants) for the uptake of radionuclides such as $^{137}$Cs by mycorrhizal fungi associated with its roots [25,26]; (iii) and *Chenopodium vulvaria* L. (7 plants) and (iv) *Chenopodium album* L. (4 plants) due to their use as fodder in livestock feed as well as their medicinal applications as anti-inflammatory agents [27]. The 25 sampled plants were collected from the sampling points shown in Figure 1.

**Figure 2.** Various stages of the soil and plant sampling and preparation process: (**a**) the waste rock dump of the "Antigua Pilar" copper mine, (**b**) a detailed view of the minerals present in the study area, (**c**) in-situ measurements taken prior to sample collection, (**d**) soil sampling using a 20 cm × 20 cm × 5 cm depth grid, (**e**) a microwave oven (Milestone, ultraWAVE, Italy) and an ball mill (FRITSCH, Pulverisette 5, Germany), and (**f**) amuffle furnace (HOBERSAL, 2003741, Spain) and alpha spectrometry measurement equipment (Mirion Canberra, Alpha Analyst, Bretonneux, France).

### 2.2. *Sampling and Preparation of Soil and Plant Samples*

The plants were selected based on their location within the study area. The plants were identified by collecting the entire aerial part of each plant, which was placed in a paper bag to avoid alterations during transport to the laboratory. The roots were not used to prevent errors in the interpretation of the results due to the presence of adhered soil, which is very complex to remove [13]. Subsequently, a surface soil sample near the plant was taken using a metal grid measuring 20 cm × 20 cm and 5 cm deep (Figure 2d) until a total of 1.0 kg of soil was collected. The samples were placed in plastic bags. The plant sample and its corresponding soil were located using a GPS. The samples were taken to the laboratory, where they were air-dried for one day.

Each soil sample was then placed in a Selecta brand oven, model 2000209 (Spain), and dried at 105 °C for 24 h until a constant weight was achieved. Next, the samples were ground in an FRITSCH Pulverisette 5 planetary ball mill (Figure 2e). Subsequently, the samples were sieved using a 120 mesh sieve, achieving a particle size of 250 µm.

The plant samples were dried in an HOBERSAL oven model 2003741 (Spain) at 65 °C for 3 days, and subsequently ashed in an HOBERSAL muffle furnace model HD150PA at 450 °C for 24 h (Figure 2f).

The soil and plant samples were mineralized in a microwave oven (Milestone, ultraWAVE, Italy) (Figure 2e). Three aliquots of 0.2 g of sample were introduced into 3 Teflon vials to which 1 mL of HF, 1 mL of $HNO_3$, and 4 mL of HCl were added. The three aliquots obtained after mineralizing each sample were added to a Teflon beaker and evaporated to dryness. Subsequently, the HF was removed by dissolving the residue with 3 mL of concentrated HCl and evaporating the solution to dryness again. This step was repeated twice. The tracers used to determine the chemical yield of the radiochemical methods were (i) $^{229}$Th solution with an activity concentration of $20.96 \pm 0.16$ Bq $g^{-1}$ (supplied by the National Laboratory of Metrology of Ionising Radiations (LMRI) of the Centre for Energy, Environmental and Technological Research (CIEMAT), Madrid, Spain) and (ii) 232U solution of $13.54 \pm 0.16$ Bq $g^{-1}$ supplied by the LRMI. The $Ba^{2+}$ carrier had a concentration of 10 mg $mL^{-1}$ and was prepared from $BaCl_2 \cdot 2H_2O$ (Merck, Germany) with analytical grade purity. The tracers were diluted with $HNO_3$ 1:100 ($v/v$) to obtain the required activity concentration for the radiochemical methods employed.

### 2.3. Determination of the Chemical Composition of Soil and Plant Samples

The chemical composition of the soil and plants was determined using a Malvern-PANanalytical AXIOS spectrophotometer. The samples were prepared using a planetary ball mill, and the samples prepared in Section 2.2 were again sieved to a particle size of 74 µm with a 200 mesh sieve. The determination of the concentration of stable cations by WDXRF was performed using a semi-quantitative method developed by Malvern-Panalytical. This method uses fundamental parameters for quantification, with a minimum of one standard per element that ensures an accuracy of at least 1%. The use of this method allows for the same aliquot to be used for subsequent radiochemical analyses, also avoiding its handling. For this purpose, the samples were placed in a special container that permits the analysis of the sample in a He atmosphere. The WDXRF technique is very stable and does not require recalibration for each sample measured since the standard deviation is very low. On the other hand, although WDXRF is capable of quantifying the uranium present in the samples, these results have not been used as they are much less sensitive and reproducible than those determined using radiochemical methods.

### 2.4. Radiochemical Methods for the Separation of $^{238}$U and $^{226}$Ra

#### 2.4.1. $^{238}$U Separation Method

The radiochemical separation method for $^{238}$U consisted of a liquid–liquid extraction with TBP dissolved in xylene in a 1:4 ($v/v$) ratio. Prior to extraction, 0.25 M EDTA solution was added to mask Th and the other cations that were co-extracted in TBP. Finally, U was re-extracted using 1 M $(NH_4)_2CO_3$ solution. The separated $^{238}$U was electrodeposited onto a stainless steel planchet using the Hallstadius method [28] (Figure 2f). The chemical yield of the method was determined from the $^{232}$U tracer described in Section 2.2. The different steps of the method used, as well as the expressions employed for the determination of the activity concentration, uncertainty, and limit of detection (LoD) of $^{238}$U, are detailed in [29]. The samples were measured for 500,000 s, achieving an LoD of $5 \cdot 10^{-3}$ Bq $kg^{-1}$ for the plant samples and 1.2 Bq $kg^{-1}$ for the soil samples.

#### 2.4.2. $^{226}$Ra Separation Method

The method used for the radiochemical separation of $^{226}$Ra was based on the co-precipitation of Ra in a $BaSO_4$ precipitate through the formation of mixed crystals. The method began with the formation of a [Pb-Ba-Ra]$SO_4$ precipitate, which was dissolved with EDTA in a strongly ammoniacal medium. The [Ba-Ra]$SO_4$ was re-precipitated with $CH_3COOH$ and transformed into [Ba-Ra]$CO_3$ using saturated $Na_2CO_3$ solution at 90 °C. Subsequently, [BaRa]$Cr_2O_7$ was precipitated to eliminate the co-precipitated alkaline earth elements (Ca, Mg, and Sr). [BaRa]$Cr_2O_7$ was transformed into [BaRa]$Cl_2$ with a HCl + $CH_3CH_2OCH_2CH_3$ mixture in a 1:6 ($v/v$) ratio. [BaRa]$Cl_2$ was dissolved in $H_2O$, and [BaRa]$SO_4$ was precipitated with 1 M $H_2SO_4$. $BaSO_4$ was filtered, deposited on a cellulose nitrate filter with a pore size of 0.45 μm, and dried to constant weight under an infrared lamp. The chemical yield of the method was determined gravimetrically from the weight of the final $BaSO_4$ obtained. A more extensive description of the method, as well as the expressions used to determine the activity concentration, uncertainty, and LoD, is detailed in [30]. The LoD obtained for the plant samples was 0.006 Bq kg$^{-1}$, and it was 0.7 Bq kg$^{-1}$ for the soil samples.

#### 2.4.3. Equipment for the Measurement of $^{238}$U and $^{226}$Ra

The stainless steel planchets with electrodeposited $^{238}$U were measured using an AlphaAnalyst model A450-18AM (Mirion Canberra, Bretonneux, France) system equipped with 12 vacuum chambers with 12 PIPS (passivated implanted planar silicon) detectors from Canberra Industries (Figure 2f). Each detector had an active area of 450 mm$^2$ and a resolution of 18 keV full width at half maximum (FWHM) at 5.486 MeV for $^{241}$Am. The spectra were acquired and analyzed using Genie 2000 software.

The [BaRa]$SO_4$ precipitates were measured using 6 ZnS(Ag) detectors. These detectors detect the light emitted when an alpha particle interacts with the ZnS(Ag) deposited on one side of a transparent plastic. This plastic was placed over the filter containing the [BaRa]$SO_4$ precipitate. The detection of the scintillations was carried out with a photomultiplier tube (Canberra model 2007P) whose signal was amplified with a Canberra model 2007A amplifier, which, in turn, was powered by a Canberra model NHQ 202M high voltage source.

### *2.5. Determination of Transfer Factors*

The transfer factors (*TFs*, kg kg$^{-1}$) were determined as the ratio between the activity concentration or chemical concentration in the dry mass of a radionuclide or stable element in the plant and in the soil using the following expression [6]:

$$TF = \frac{C_{plant(d.m.)}}{C_{soil(d.m.)}} \tag{1}$$

where $C_{plant(d.m.)}$ is the activity concentration of a radionuclide ($^{238}$U and $^{226}$Ra) or a stable element in the plant (dry mass), and $C_{soil(d.m.)}$ is the activity concentration of a radionuclide ($^{238}$U and $^{226}$Ra) or a stable element in the soil (dry mass). The uncertainty associated with the transfer factor (u(TF), Bq kg$^{-1}$) is determined by the following expression:

$$u(TF) = TF \cdot \sqrt{\left(\frac{u\left(C_{plant(d.m.)}\right)}{C_{plant(d.m.)}}\right)^2 + \left(\frac{u\left(C_{soil(d.m.)}\right)}{C_{soil(d.m.)}}\right)^2} \tag{2}$$

### *2.6. Statistical Analysis of Results*

Various statistical analyses conducted in this study were carried out using the RStudio statistical software version 2024.04.2 Build 764, utilizing the following libraries: *stats*, *car*, *writexl*, *psych*, *FactomineR*, and *Factoextra*. The statistical analyses performed are summarized below.

Firstly, principal component analysis (hereafter, PCA) was conducted, through which the samples were grouped based on variables with an influence above the average value of the entire set of variables. Additionally, it was verified that the selected variables had a Kaiser–Meyer–Olkin parameter value above 0.5 [31].

Subsequently, multiple linear regression analysis (MLRA) was performed to verify that the variables obtained in PCA had statistical significance and to obtain a model relating the incorporation of $^{238}U$ and $^{226}Ra$ with the incorporation of stable elements. The variables used in the models did not exhibit collinearity among them, a factor that was verified using the Variance Inflation Factor (VIF). Finally, the weight of the model parameters allowed us to draw conclusions from this study, selecting those with the highest values of the standardized coefficients as the most influential. The standardized coefficients were determined by transforming the model coefficients using their standard deviation [23].

## 3. Results and Discussion

### *3.1. Chemical Composition of Soil Samples*

Figure 3 shows box-and-whisker plots, illustrating the concentrations of different stable elements in the soil samples. The data indicate that $SiO_2$ is the principal compound, followed by these other major elements: Al, Ca, Fe, K, P, and Mg. Cu, Mn, S, and Ti were the predominant elements with higher percentages. The concentrations of the major elements, namely O, Si, Al, Ca, Fe, K, P, and Mg, were equivalent to those typically found in soil samples [32]. Cu had an average concentration of 1600 mg kg$^{-1}$, which is significantly higher than the European average value of 35.3 mg kg$^{-1}$ in unimpacted soils [33] and 496.3 mg kg$^{-1}$ in soils contaminated by pesticides [34]. However, the levels found were consistent with those in other areas affected by Cu mining, where a value of 1600 mg kg$^{-1}$ was also obtained [35]. Sulphur also showed values well above the average in soils of 24.6 mg kg$^{-1}$. On the other hand, the As value was consistent with that obtained in other studies on soils affected by U mining, whose average value of 233 mg kg$^{-1}$ is equivalent to the one obtained in this work of 303 mg kg$^{-1}$ [36]. The elements identified were consistent with the mineral species characteristic of a copper mine tailings site. On the one hand, Cu is associated with chalcopyrite ($CuFeS_2$), bornite ($Cu_{1.8}Fe_{1.2}S_4$), and chalcocite ($Cu_2S$) [37]. Mn is a part of pyrolusite ($MnO_2$); Fe is found in hematite ($Fe_2O_3$), pyrite ($FeS_2$), and magnetite ($Fe_3O_4$); and Ti is found in rutile or ilmenite ($FeTiO_3$) [38]. The trace elements found were also consistent with those typically encountered in such tailings [39]: (i) As as arsenopyrite (FeAsS), (ii) Zn as sphalerite (ZnS), (iii) Ba as barite ($BaSO_4$) and witherite ($BaCO_3$), and Cr due to the presence of chromite ($FeCr_2O_4$).

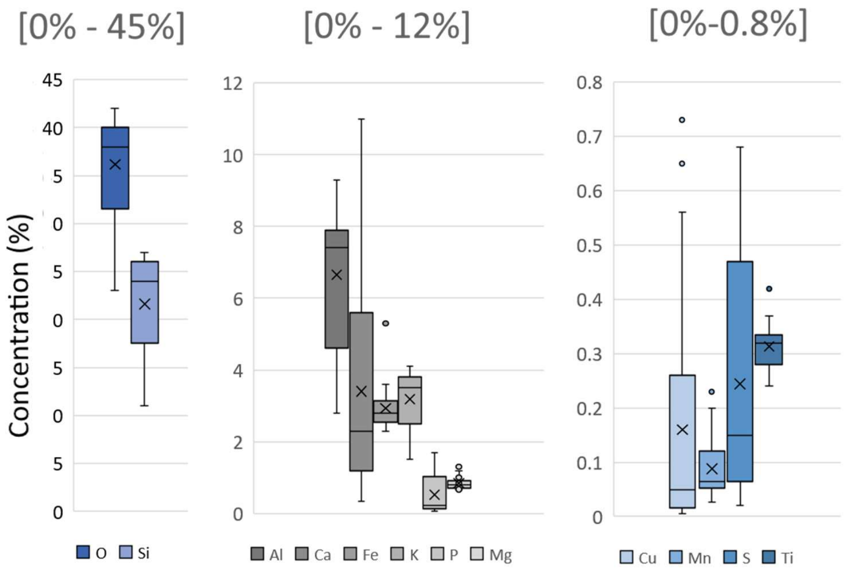

**Figure 3.** *Cont.*

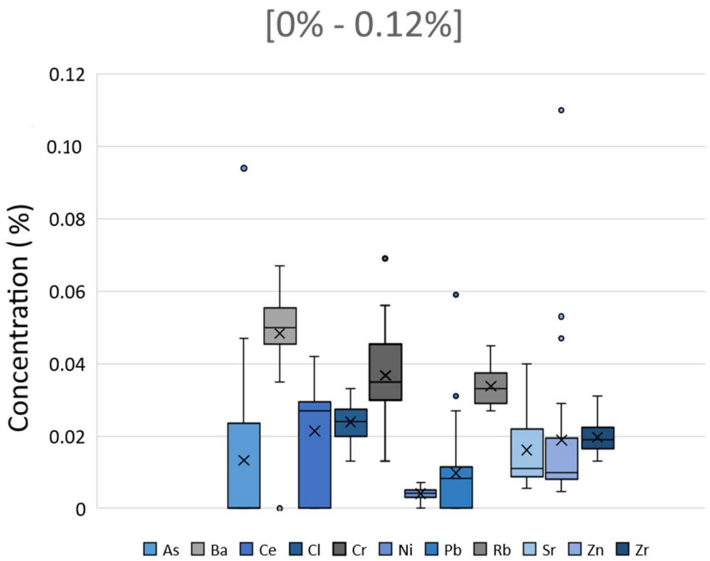

**Figure 3.** The chemical composition of the soils sampled in this study. The values are presented in Tables S1–S8 of the Supplementary Information.

### 3.2. Activity Concentration Values of $^{238}$U and $^{226}$Ra

Table 1 shows the activity concentration results of $^{238}$U and $^{226}$Ra in the 25 sampled soils, whose values were higher than the average value for Spanish soils of 30 Bq kg$^{-1}$ [40]. The elevated presence of $^{238}$U and $^{226}$Ra is due to the hydrothermal formation of the study area, which caused a significant increase in uranium radioactive series [41]. This presence is primarily due to the presence of torbernite ($Cu(UO_2)_2(PO_4)_2 \cdot 8–12H_2O$) in the area, as described in Section 2.1. Figure 4 shows the activity concentration of $^{226}$Ra as a function of the activity concentration of $^{238}$U. The ratio of $^{226}$Ra/$^{238}$U was obtained from the slope of the linear equation, with a value of 1.237 ± 0.065. The obtained ratio showed that U(IV) is oxidized by external agents into $UO_2^{2+}$, which is more soluble than $^{226}$Ra and is thus released into the environment through rain and air [42].

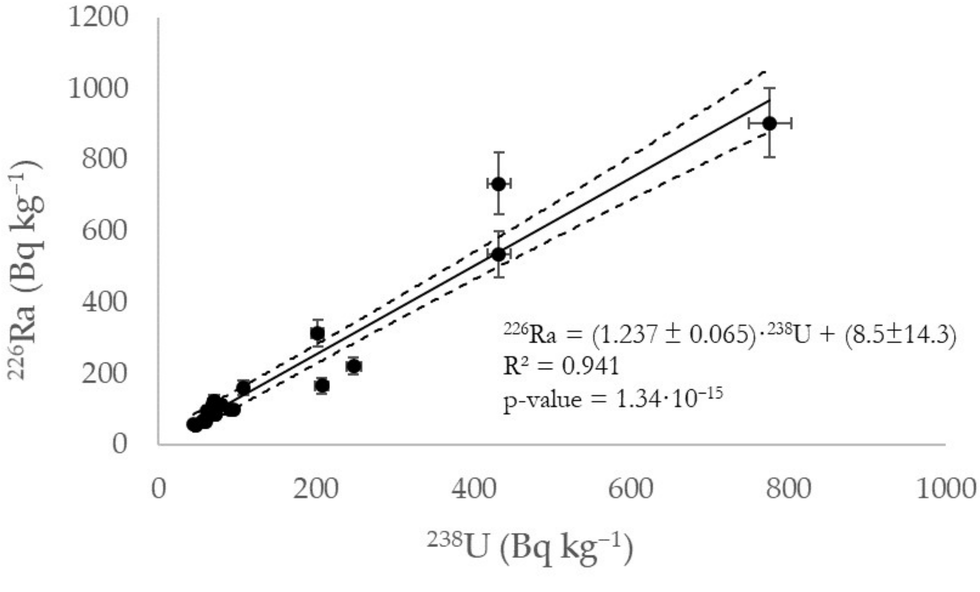

**Figure 4.** Ratio of $^{226}$Ra concentration (Bq kg$^{-1}$) to $^{238}$U (Bq kg$^{-1}$) (the dotted line corresponds to the confidence intervals of the function).

**Table 1.** The activity concentrations of $^{238}$U and $^{226}$Ra for the 25 plants and soils together with the soil–plant transfer factors.

| | | **Soil (Bq kg$^{-1}$)** | | **Plant (Bq kg$^{-1}$)** | | **Transfer Factors (kg kg$^{-1}$)** | |
|---|---|---|---|---|---|---|---|
| **Species** | **Sample** | **$^{238}$U** | **$^{226}$Ra** | **$^{238}$U** | **$^{226}$Ra** | **$^{238}$U** | **$^{226}$Ra** |
| *Scolymus Hispanicus* L. | 1 | 79.3 ± 3.7 | 113 ± 13 | 0.232 ± 0.067 | 4.03 ± 0.50 | 0.00293 ± 0.00086 | 0.0357 ± 0.0060 |
| | 2 | 107.6 ± 4.6 | 161 ± 20 | 0.232 ± 0.058 | 1.40 ± 0.21 | 0.00216 ± 0.00055 | 0.0087 ± 0.0017 |
| | 3 | 247.5 ± 9.1 | 222 ± 23 | 0.73 ± 0.11 | 3.93 ± 0.45 | 0.00295 ± 0.00046 | 0.0177 ± 0.0027 |
| | 4 | 68.6 ± 2.9 | 117 ± 13 | 0.402 ± 0.073 | 0.73 ± 0.14 | 0.0059 ± 0.0011 | 0.0062 ± 0.0014 |
| | 5 | 70.6 ± 2.8 | 125 ± 15 | 0.196 ± 0.059 | 1.34 ± 0.19 | 0.00278 ± 0.00084 | 0.0107 ± 0.0020 |
| | 6 | 432 ± 15 | 735 ± 88 | 0.332 ± 0.076 | 3.07 ± 0.38 | 0.00077 ± 0.00018 | 0.00418 ± 0.00072 |
| | 7 | 70.2 ± 3.1 | 122 ± 13 | 0.101 ± 0.053 | 1.55 ± 0.23 | 0.00144 ± 0.00076 | 0.0127 ± 0.0023 |
| | 8 | 776 ± 27 | 904 ± 97 | 0.467 ± 0.094 | 3.55 ± 0.52 | 0.00060 ± 0.00012 | 0.00393 ± 0.00071 |
| | 9 | 432 ± 15 | 537 ± 65 | 0.153 ± 0.095 | 1.57 ± 0.22 | 0.00035 ± 0.00022 | 0.00292 ± 0.00054 |
| *Eryngium Campestre* L. | 10 | 65.0 ± 2.5 | 93 ± 11 | 0.328 ± 0.062 | 0.92 ± 0.18 | 0.00505 ± 0.00097 | 0.0099 ± 0.0023 |
| | 11 | 58.9 ± 2.3 | 64.6 ± 7.3 | 0.071 ± 0.027 | 1.17 ± 0.17 | 0.00121 ± 0.00046 | 0.0181 ± 0.0033 |
| | 12 | 54.5 ± 2.3 | 65.1 ± 8.3 | 0.091 ± 0.030 | 1.12 ± 0.16 | 0.00167 ± 0.00055 | 0.0172 ± 0.0033 |
| | 13 | 55.9 ± 2.3 | 68.1 ± 8.8 | 0.143 ± 0.044 | 0.80 ± 0.12 | 0.00256 ± 0.00079 | 0.0117 ± 0.0023 |
| | 14 | 47.0 ± 2.0 | 55.6 ± 6.9 | 0.064 ± 0.033 | 2.20 ± 0.28 | 0.00136 ± 0.00070 | 0.0396 ± 0.0070 |
| *Chenopodium Vulvaria* L. | 15 | 44.6 ± 2.3 | 59.3 ± 6.9 | 0.35 ± 0.11 | 0.093 ± 0.032 | 0.0078 ± 0.0025 | 0.00157 ± 0.00057 |
| | 16 | 61.5 ± 2.7 | 98 ± 11 | 0.0189 ± 0.0075 | 2.89 ± 0.72 | 0.00031 ± 0.00012 | 0.0295 ± 0.0081 |
| | 17 | 71.4 ± 3.1 | 87 ± 10 | 0.059 ± 0.057 | 0.016 ± 0.012 | 0.00083 ± 0.00080 | 0.00018 ± 0.00014 |
| | 18 | 66.7 ± 3.2 | 105 ± 12 | 0.181 ± 0.069 | 2.97 ± 0.58 | 0.0027 ± 0.0010 | 0.0283 ± 0.0064 |
| | 19 | 60.1 ± 3.1 | 73.1 ± 7.4 | 0.112 ± 0.058 | 0.63 ± 0.26 | 0.00186 ± 0.00097 | 0.0086 ± 0.0037 |
| | 20 | 207.2 ± 7.9 | 167 ± 23 | 0.104 ± 0.073 | 1.07 ± 0.78 | 0.00050 ± 0.00035 | 0.0064 ± 0.0048 |
| | 21 | 202.3 ± 7.7 | 315 ± 37 | 0.068 ± 0.052 | 0.37 ± 0.18 | 0.00034 ± 0.00026 | 0.00117 ± 0.00059 |
| *Chenopodium Album* L. | 22 | 90.3 ± 3.8 | 100 ± 10 | 0.070 ± 0.062 | 0.54 ± 0.35 | 0.00078 ± 0.00069 | 0.0054 ± 0.0035 |
| | 23 | 71.4 ± 3.1 | 87 ± 10 | 0.0110 ± 0.0057 | 1.03 ± 0.79 | 0.000154 ± 0.000080 | 0.0118 ± 0.0092 |
| | 24 | 62.8 ± 2.9 | 88 ± 10 | 0.0095 ± 0.0017 | 0.22 ± 0.11 | 0.000151 ± 0.000028 | 0.0025 ± 0.0013 |
| | 25 | 94.7 ± 3.9 | 101 ± 11 | 0.069 ± 0.043 | 0.56 ± 0.27 | 0.00073 ± 0.00046 | 0.0055 ± 0.0027 |

The uncertainties are quoted for a coverage factor k = 2.

### *3.3. Relationship between the Chemical Composition of Soils and the Activity Concentration of $^{238}$U and $^{226}$Ra*

Figure 5 shows a biplot graph with principal component analysis (PCA) that allows for visualization of the correlation between the activity concentration of $^{238}$U and $^{226}$Ra and the chemical composition and scoring of the different soils based on these variables. The two factors obtained represent 90.4% of the variance, indicating statistical dependence between the different variables. The Kaiser–Meyer–Olkin (KMO) index value was 0.79, which indicates a satisfactory correlation [43]. Some variables were eliminated as they did not exceed the average contribution of the set of variables or 1/(number of variables). The correlation between the different variables is obtained from the cosine of the angle they form with each other. The results showed a correlation between the activity concentrations of $^{226}$Ra and $^{238}$U with Sn, Fe, and Cu. This results indicate that the radionuclides were associated with areas with higher mineral content from the waste heap. Soils 8, 6, 3, 9, 2, and 21 are those that would have the highest content of natural radionuclides, with soil 8 standing out. These soils are located in the waste heap and the mine loading area, which, as verified in a previous study, had the highest radioactive content [23]. The remaining stable elements did not show any correlation with $^{238}$U or $^{226}$Ra. However, coherent correlations are observed, such as those of Si with O (due to $SiO_2$) and Na and K, which have the same chemical behavior. Additionally, a correlation was observed between Ca, Sr, and S, possibly due to the presence of sulfates, an aspect that would require further analysis to confirm. However, $^{226}$Ra is not correlated with Ca, Sr, and S, indicating that its presence is more commonly associated with U, its progenitor. Therefore, the correlation between U and Fe is consistent with the findings of other authors such as Ha et al. [44], who found that Fe-rich minerals can reduce heavy metals like U from $UO_2^{2+}$, the most soluble species, to U(IV), which is less soluble. Furthermore, the subsequent formation of Fe oxyhydroxides such as ferrihydrite would favor the release of U under high-temperature conditions, which is consistent with the meteorological conditions of the study area [45,46].

The presence of carbonate would also favor the release of U from the oxyhydroxides [47], which, as verified in a previous study, is a significant fraction in the tailings [48]. Therefore, the formation of oxyhydroxides would explain the $^{238}$U/$^{226}$Ra ratio shown in Figure 3.

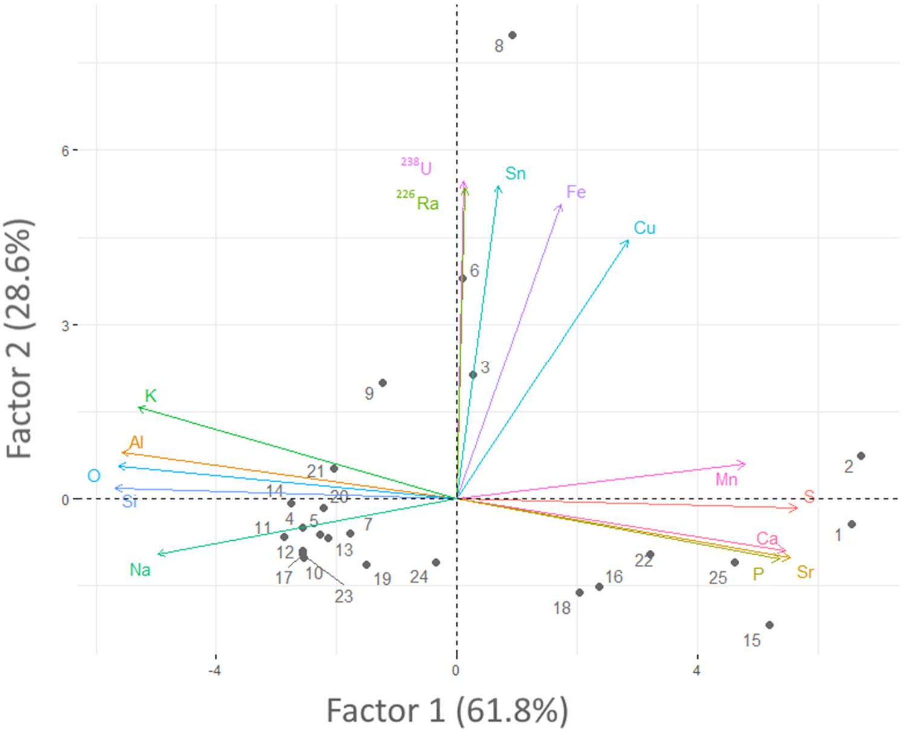

**Figure 5.** A biplot graph showing the correlation between the concentration of $^{226}$Ra (Bq kg$^{-1}$) and $^{238}$U (Bq kg$^{-1}$) and the chemical composition, along with the scoring of the different soils studied based on these variables. The data used to construct this graph are found in Tables S1–S8 of the Supplementary Information.

Another observed aspect was the qualitative relationship between the presence of As and $^{238}$U, as they are usually associated in this type of deposit [49]. However, the data did not show any correlation. Therefore, the presence of As would only indicate that the samples were taken from the tailings and the mineral loading area (soils 1, 2, 3, 5, 7, 8, 9, 17, 22, 23, and 25).

### 3.4. Transfer Factors of $^{238}$U and $^{226}$Ra between Soil and Studied Plants

Figure 6 shows the transfer factors (TF) of $^{226}$Ra and $^{238}$U for the four species studied. On the other hand, Figure 6 presents a biplot graph in which the TFs for $^{226}$Ra, $^{238}$U, and the stable elements (K, Mg, Fe, Al, Na, S, Ti, Ca, and Sr) are represented as variables. The range of transfer factors obtained for $^{238}$U varied between $1.5 \cdot 10^{-4}$ kg$^{-1}$ kg$^{-1}$ and $7.8 \cdot 10^{-3}$ kg$^{-1}$ kg$^{-1}$, while for $^{226}$Ra, the range was between $1.8 \cdot 10^{-4}$ kg$^{-1}$ kg$^{-1}$ and $4.0 \cdot 10^{-2}$ kg$^{-1}$ kg$^{-1}$. The ranges obtained for the transfer factors of $^{238}$U and $^{226}$Ra were similar to those observed in semi-arid climates [12,18,50,51]. Furthermore, these transfer factors were also comparable to those found in mine tailings present in semi-arid climates [16]. Moreover, the transfer factors followed a logical pattern, with those obtained for $^{226}$Ra being higher than those for $^{238}$U [52]. The elements represented in the graph were those that exceeded the average contribution, as shown in the biplot graph of Figure 4. The KMO index was 0.54, which is low, but represents 57.3% of the variance and is higher than the value of 0.5 necessary to obtain statistically representative results [31]. The TFs obtained for $^{226}$Ra and $^{238}$U are consistent with those obtained by other authors in areas impacted and not impacted by U mining, which ranged between $2 \cdot 10^{-4}$ and 0.1 kg kg$^{-1}$, whose characteristics are equivalent to those of the samples analyzed in this study [7,8,31,53,54].

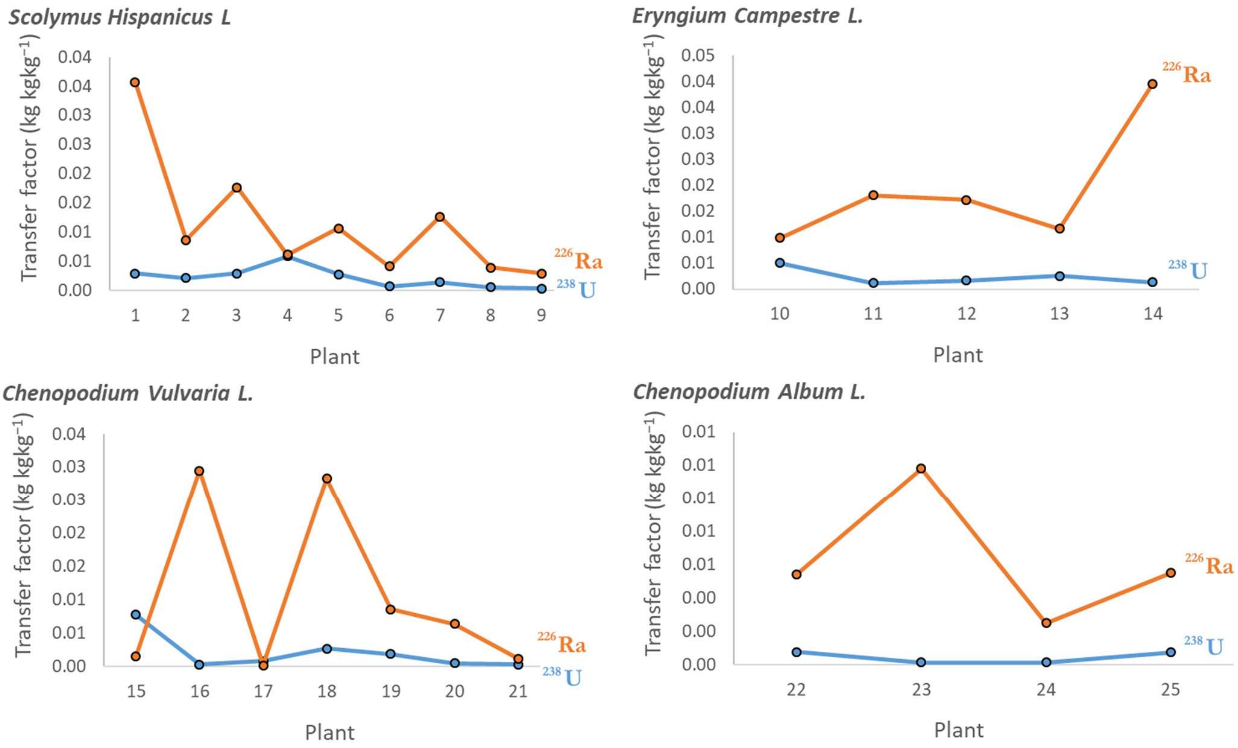

**Figure 6.** The transfer factors for $^{226}$Ra and $^{238}$U for the four plant species studied.

The biplot graph clearly shows four data sets directly related to the species studied (Figure 7). The species *Chenopodium vulvaria* L. and *Chenopodium album* L. are the ones least related to the radioactive content of the soils, as the angle formed by the variables $^{238}$U and $^{226}$Ra is 90°, indicating no correlation. These plants are associated with the incorporation of K and Mg. K is often associated with a greater presence of mycorrhizal fungi, as confirmed by other authors such as El-Mesbahi et al. [55]. The presence of mycorrhizal fungi is, in turn, associated with less U absorption, as demonstrated in the previous studies [56]. Similarly, the incorporation of Mg is related to the reduced incorporation of $^{137}$Cs and $^{226}$Ra due to the competition of Mg for accessible positions in the soil [57]. The reduced incorporation of K and Mg by *Scolymus hispanicus* L. and *Eryngium campestre* L. imply a greater incorporation of $^{226}$Ra mainly. On the other hand, the presence of Ti is related to the absorption of $^{226}$Ra, as it favors its mobility; thus, increasing the incorporation of Ti would increase that of $^{226}$Ra [58]. The results also show how the incorporation of $^{226}$Ra is related to the incorporation of Ca and Sr due to their similar behaviors. However, as previously mentioned, Mg, although it is an alkaline earth metal, competes with these cations. Therefore, the incorporation of $^{226}$Ra is coherent from the perspective of Mg, Ca, and Sr. Regarding U, the results showed that its content is greater in the case of *Scolymus hispanicus* L. and this is associated with the incorporation of other heavy metals such as Fe and Al. The relationship between U, Fe, and Al was observed in the previous studies of granites [59], and it is consistent with the type of soil in the study area (see Section 2.1). Finally, the incorporation of $^{238}$U and $^{226}$Ra did not show any correlation with each other, as the angle of these two variables is practically 90°. This effect is consistent with the TFs obtained for these two elements (Figure 4). The results obtained show that both *Scolymus Hispanicus* L. and *Eryngium Campestre* L. are the plants that absorb the most $^{238}$U and $^{226}$Ra, along with other heavy metals such as Fe and Al. *Scolymus Hispanicus* L. has the ability to alter the soil as its roots generate organic acids and sugars that lead to an increase in pH, the formation of chelates with heavy metals, and an increase in the presence of microorganisms [24]. *Eryngium Campestre* L. exhibits a high level of mycorrhization in its roots, which also promotes the greater mobility of $^{238}$U and $^{226}$Ra, as well as heavy metals, enhancing their incorporation into the plant [25]. Although future research is necessary to validate these hypotheses, the correlation with sulfur present in the composition of minerals found in a copper tailings site (see Section 3.1.) indicate the possible decomposition of the sulfides present. Therefore, these two plants could be candidates for use in phytoremediation.

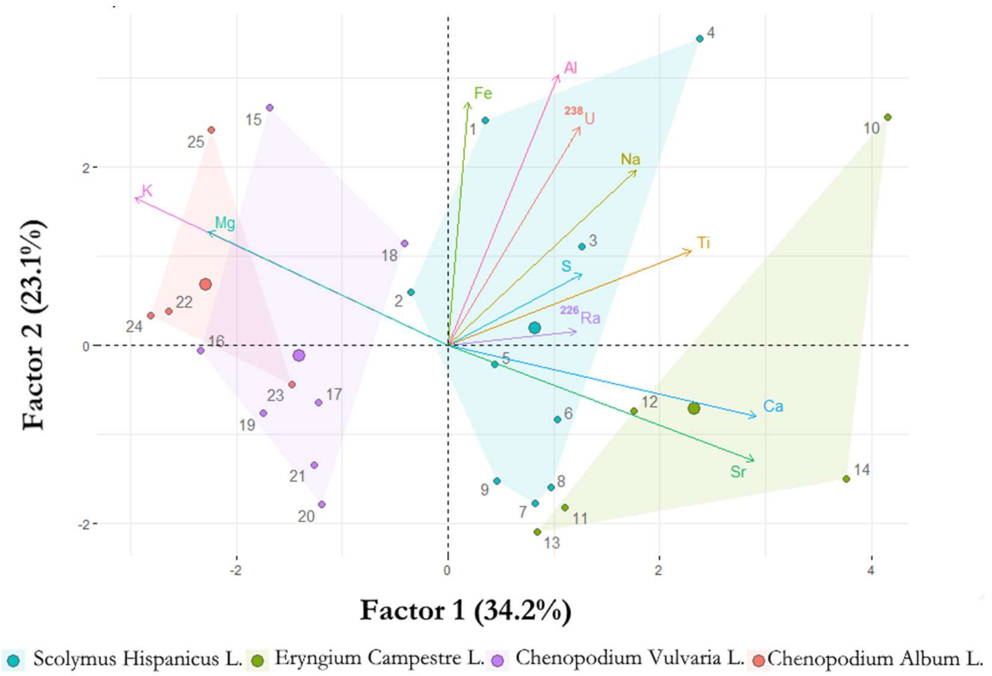

**Figure 7.** A biplot graph relating the transfer factors of $^{238}$U and $^{226}$Ra with those of the stable elements K, Mg, Fe, Al, Na, S, Ti, Ca, and Sr for the four plant species studied.

### *3.5. General Model of Transfer of $^{238}$U and $^{226}$Ra Based on the Transfer of Stable Elements*

The transfer models of $^{238}$U and $^{226}$Ra obtained through multiple linear regression analysis have the following equations:

$$TF_{^{238}U} = (1.84 \pm 0.49) \cdot TF_{Al} + (0.00024 \pm 0.0001) \cdot TF_{S} - (0.00066 \pm 0.00069) \tag{3}$$

$$\begin{aligned} TF_{^{226}Ra} = {} & (10.0 \pm 4.6) \cdot TF_{Al} + (0.0036 \pm 0.0014) \cdot TF_{Ca} - (4.2 \pm 2.0) \cdot TF_{Fe} + (0.016 \pm 0.010) \cdot TF_{Mg} - \cdots \\ & \cdots - (0.62 \pm 0.30) \cdot TF_{Na} + (1.72 \pm 0.84) \cdot TF_{Ti} + (0.0032 \pm 0.0074) \end{aligned} \tag{4}$$

The residuals obtained through the proposed models for $^{238}$U and $^{226}$Ra were evaluated using RSE and RMSE statistics, yielding $1.5 \cdot 10^{-4}$ and $1.5 \cdot 10^{-4}$ for $^{238}$U and $8.8 \cdot 10^{-3}$ and $7.4 \cdot 10^{-3}$ for $^{226}$Ra. Therefore, the values estimated by the models yield consistent results. The models were simplified by eliminating the parameters with a *p*-value greater than 0.05 in the analysis of variance. The weight of the most influential factors in the absorption of $^{238}$U and $^{226}$Ra was determined by examining the standard coefficients of the fit. The parameter that had the greatest weight in the fit for $^{238}$U was Al, while for $^{226}$Ra, it was Al >> Fe > Ti. The interaction observed between $^{238}$U and Al may be equivalent to that found by Bachmaf and Merkel [60], who observed an interaction between Al and $UO_2^{2+}$ in clay samples due to available sites on the surface where Al was present. This same effect was found by Yamaguchi et al. in clays [61]. Although the interactions between $^{238}UO_2^{2+}$ and $^{226}Ra^{2+}$ with $Al^{3+}$ were found in the clay samples, they are extrapolable to soils due to their similar behaviors. Therefore, the absorption of $^{238}$U and $^{226}$Ra is related to that of Al and is directly proportional since the sign found in the model is positive. A relationship between $^{226}$Ra and Fe and Ti has been found in previous studies on granite samples [61]. The interaction of Ti with $^{226}$Ra, according to our results, is positive, which is equivalent to the results obtained by Rubinos and Barral [58]. On the other hand, the negative relationship found between $^{226}$Ra and Fe is due to the presence of a high concentration of Fe, as is the case with the soils in the study area, which can influence the mobility of $^{226}$Ra as it forms complexes with $Fe_2O_3$ that prevent its absorption by plants [62]. The proposed models emphasize the significance of mycorrhization in the uptake of radionuclides and heavy metals by plants [63–65]. The microorganisms present in the roots play a crucial role in the mobility of $^{238}$U and $^{226}$Ra, as well as Fe and Al, due to pH variation and chelate formation [24]. The microorganisms may induce the chemical dissociation of the compounds formed by $^{238}$U with Al and Fe and by $^{226}$Ra with S and Ti. These mechanisms need to be investigated and confirmed in future studies on the transfer factors of radionuclides under arid and semi-arid conditions.

## 4. Conclusions

The results obtained have allowed us to verify our working hypothesis that the incorporation of $^{238}$U and $^{226}$Ra in a climate similar to a semi-arid one is related to that of stable elements.

The study area was characterized by the high presence of radionuclides from uranium and actinium series, along with Cu and Fe values well above the global values for soils. Despite the complexity of this type of soil and the similarity of the climate in the study area to a semi-arid climate, no different TFs were obtained compared to those of areas with different climates, such as tropical ones. The range of transfer factors for $^{238}$U varied between $1.5 \cdot 10^{-4}$ kg$^{-1}$ kg$^{-1}$ and $7.8 \cdot 10^{-3}$ kg$^{-1}$ kg$^{-1}$, while for $^{226}$Ra, the range was between $1.8 \cdot 10^{-4}$ kg$^{-1}$ kg$^{-1}$ and $4.0 \cdot 10^{-2}$ kg$^{-1}$ kg$^{-1}$. Likewise, in addition to the values obtained for the TFs, the behavior of the natural radionuclides in relation to the stable elements, mainly K, Mg, Ca, Fe, and Ti, is similar to those observed in the literature. The results showed how K and Mg lead to the reduced incorporation of $^{238}$U and $^{226}$Ra due to the possible presence of mycorrhizal fungi, resulting from the greater incorporation of K and also competition between Mg and the remaining alkaline earth metals (Ra, Ca, and Sr). The presence of arbuscular mycorrhizal fungi has not been verified, and this conclusion is based on the results of previous studies; however, a count of arbuscular mycorrhizal fungi vesicles is necessary to ensure this conclusion. Furthermore, the mobility of $^{226}$Ra is related to the presence of Ti, an aspect observed by the $^{226}$Ra/Ti correlation in the biplot graph representing the TFs. Finally, the incorporation of U showed the expected behavior and correlated with the presence of Fe and Al typical of granitic soils like that of the study area.

The correlations found were consistent with the parameters with the most weight in the absorption models of $^{238}$U and $^{226}$Ra. The interaction between Al and $^{238}$U and $^{226}$Ra was similar to that observed in clays, showing a positive relationship between them. On the other hand, Ti facilitates the movement of $^{226}$Ra, which matched the positive relationship in the model. Finally, Fe retains Ra by forming a complex with $Fe_2O_3$ when there is a high concentration of Fe, an aspect that is consistent with the levels found in the study area. Our results indicate that both *Scolymus hispanicus* L. and *Eryngium campestre* L. could be utilized in the phytoremediation of soils contaminated by natural radionuclides in semi-arid climates. Therefore, our results have confirmed that there is a significant relationship between the incorporation of stable and radioactive elements, which helps in understanding the absorption mechanisms of plants under conditions similar to a semi-arid climate.

**Supplementary Materials:** The following supporting information can be downloaded at: https://www.mdpi.com/article/10.3390/app14209201/s1, Table S1: Chemical composition of soils associated with *Scolymus Hispanicus* L., as determined by X-Ray Fluorescence; Table S2: Chemical composition of soils associated with *Eryngium Campestre* L., as determined by X-Ray Fluorescence, Table S3: Chemical composition of soils associated with *Chenopodium Vulvaria* L., as determined by X-Ray Fluorescence; Table S4: Chemical composition of soils associated with *Chenopodium Album* L., as determined by X-Ray Fluorescence; Table S5: Chemical composition of *Scolymus Hispanicus* L., as determined by X-Ray Fluorescence; Table S6: Chemical composition of *Eryngium Campestre* L., as determined by X-Ray Fluorescence; Table S7: Chemical composition of *Chenopodium Vulvaria* L., as determined by X-Ray Fluorescence; Table S8: Chemical composition of *Chenopodium Album* L., as determined by X-Ray Fluorescence.

**Author Contributions:** Conceptualization, J.A.S.-N. and V.M.E.-S.; methodology, J.A.S.-N., V.M.E.-S., M.B.G.-M. and M.M.-Q.; validation, J.A.S.-N. and V.M.E.-S.; formal analysis, J.A.S.-N.; investigation, J.A.S.-N., V.M.E.-S. and M.B.G.-M.; resources, M.M.-Q., M.B. and M.C.; data curation, J.A.S.-N. and V.M.E.-S.; writing—original draft preparation, J.A.S.-N.; writing—review and editing, V.M.E.-S. and J.F.B.; supervision, J.A.S.-N. and V.M.E.-S. All authors have read and agreed to the published version of the manuscript.

**Funding:** This study was funded by the Spanish Ministry of Science and Innovation as part of the internal CIEMAT project "Caracterización Radiológica y Dosimétrica de terrenos en la Comunidad de Madrid" (353-M_CU_PILAR).

**Data Availability Statement:** The original contributions presented in the study are included in the article/Supplementary Material, further inquiries can be directed to the corresponding author.

**Conflicts of Interest:** The authors declare no conflicts of interest.

## References

1. Al-Hamarneh, I.F.; Alkhomashi, N.; Almasoud, F.I. Study on the radioactivity and soil-to-plant transfer factor of $^{226}$Ra, $^{234}$U and $^{238}$U radionuclides in irrigated farms from the northwestern Saudi Arabia. *J. Environ. Radioact.* **2016**, *160*, 1–7. [CrossRef] [PubMed]
2. Sokolik, G.A.; Ovsiannikova, S.V.; Voinikava, K.V.; Ivanova, T.G.; Papenia, M.V. Biological availability of $^{238}$U, $^{234}$U and $^{226}$Ra for wild berries and meadow grasses in natural ecosystems of Belarus. *J. Environ. Radioact.* **2014**, *127*, 155–162. [CrossRef] [PubMed]
3. Soudek, P.; Petřík, P.; Vágner, M.; Tykva, R.; Plojhar, V.; Petrová, Š.; Vaněk, T. Botanical survey and screening of plant species which accumulate $^{226}$Ra from contaminated soil of uranium waste depot. *Eur. J. Soil Biol.* **2007**, *43*, 251–261. [CrossRef]
4. Soudek, P.; Petrová, Š.; Benešová, D.; Kotyza, J.; Vágner, M.; Vaňková, R.; Vaněk, T. Study of soil–plant transfer of $^{226}$Ra under greenhouse conditions. *J. Environ. Radioact.* **2010**, *101*, 446–450. [CrossRef]
5. *UNE EN 196-2*; Method of Testing Cement-Part 2: Chemical Analysis of Cement. AENOR: Madrid, Spain, 2014. (In Spanish)
6. Balonov, M.; Barnett, C.; Belli, M.; Beresford, N.; Berkovsky, V.; Bossew, P.; Boyer, P.; Brittain, J.; Calmon, P.; Carini, F. *Handbook of Parameter Values for the Prediction of Radionuclide Transfer in Terrestrial and Freshwater Environments*; IAEA: Vienna, Austria, 2010.
7. Vandenhove, H.; Van Hees, M. Predicting radium availability and uptake from soil properties. *Chemosphere* **2007**, *69*, 664–674. [CrossRef]
8. Chen, S.B.; Zhu, Y.G.; Hu, Q.H. Soil to plant transfer of $^{238}$U, $^{226}$Ra and $^{232}$Th on a uranium mining-impacted soil from southeastern China. *J. Environ. Radioact.* **2005**, *82*, 223–236. [CrossRef]
9. Günther, A.; Bernhard, G.; Geipel, G.; Reich, T.; Roßberg, A.; Nitsche, H. Uranium speciation in plants. *Radiochim. Acta* **2003**, *91*, 319–328. [CrossRef]
10. Vandenhove, H.; Van Hees, M.; Wouters, K.; Wannijn, J. Can we predict uranium bioavailability based on soil parameters? Part 1: Effect of soil parameters on soil solution uranium concentration. *Environ. Pollut.* **2007**, *145*, 587–595. [CrossRef]
11. Zakaly, H.M.H.; Awad, H.A.; Lasheen, E.S.R.; Issa, S.A.M.; Elsaman, R.; Khandaker, M.U.; Al-awah, H.; Fathy, D.; Sami, M. Radiometric and petrographic characterization of El-Yatima granite: Evaluating radiological risks and mineralogical features. *Radiat. Phys. Chem.* **2024**, *224*, 111992. [CrossRef]
12. Rea, M.A.D.; Johansen, M.P.; Payne, T.E.; Hirth, G.; Hondros, J.; Pandelus, S.; Tucker, W.; Duff, T.; Stopic, A.; Green, L.; et al. Radionuclides and stable elements in vegetation in Australian arid environments: Concentration ratios and seasonal variation. *J. Environ. Radioact.* **2021**, *234*, 106627. [CrossRef]
13. Vera Tome, F.; Blanco Rodríguez, M.P.; Lozano, J.C. Soil-to-plant transfer factors for natural radionuclides and stable elements in a Mediterranean area. *J. Environ. Radioact.* **2003**, *65*, 161–175. [CrossRef] [PubMed]
14. Semioshkina, N.; Voigt, G. Soil–Plant transfer of radionuclides in arid environments. *J. Environ. Radioact.* **2021**, *237*, 106692. [CrossRef] [PubMed]
15. Al-Masri, M.S.; Amin, Y.; Khalily, H.; Al-Masri, W.; Al-Khateeb, Y. Assessment of natural radionuclide transfer factors and partition coefficients in some Syrian soils. *J. Environ. Radioact.* **2021**, *229–230*, 106538. [CrossRef]
16. Fernandes, H.M.; Lamego Simoes Filho, F.F.; Perez, V.; Franklin, M.R.; Gomiero, L.A. Radioecological characterization of a uranium mining site located in a semi-arid region in Brazil. *J. Environ. Radioact.* **2006**, *88*, 140–157. [CrossRef] [PubMed]
17. Duong, V.H.; Nguyen, T.D.; Kocsis, E.; Csordas, A.; Hegedus, M.; Kovacs, T. Transfer of radionuclides from soil to Acacia auriculiformis trees in high radioactive background areas in North Vietnam. *J. Environ. Radioact.* **2021**, *229–230*, 106530. [CrossRef]
18. Misdaq, M.A.; Chaouqi, A. Study of the transfer of $^{238}$U, $^{232}$Th and $^{222}$Rn radionuclides from soil to cereal plants and root vegetables in a semi-arid area: Resulting radiation doses to rural consumers. *Appl. Radiat. Isot.* **2023**, *201*, 111015. [CrossRef]
19. Al-Oudat, M.; Al Attar, L.; Othman, I. Transfer factor of $^{137}$Cs and $^{90}$Sr to various crops in semi-arid environment. *J. Environ. Radioact.* **2021**, *228*, 106525. [CrossRef]
20. Salminen-Paatero, S.; Paatero, J. Transfer of Natural Radionuclides in Terrestrial Food Chains—A Review of Investigations in Finland. *Int. J. Environ. Res. Public Health* **2021**, *18*, 10577. [CrossRef]

21. Navas, M.; Pérez-Esteban, J.; Torres, M.-A.; Hontoria, C.; Moliner, A. Taxonomic and functional analysis of soil microbial communities in a mining site across a metal(loid) contamination gradient. *Eur. J. Soil Sci.* **2021**, *72*, 1190–1205. [CrossRef]
22. Martin-Izard, A.; Arribas, A.; Arias, D.; Ruiz, J.; Fernández, F.J. The Fe deposit, West-Central Spain: Tectonic-Hydrothermal uranium mineralization associated with transpressional faulting of alpine age. *Can. Miner.* **2002**, *40*, 1505–1520. [CrossRef]
23. Expósito-Suárez, V.M.; Suárez-Navarro, J.A.; Caro, A.; Sanz, M.B.; Hernaiz, G.; González-Sanabria, A.; Suárez-Navarro, M.J.; Jordá-Bordehore, L.; Chamorro-Villanueva, H.; Arlandi, M.; et al. Radiological characterization of the tailings of an abandoned copper mine using a neural network and geostatistical analysis through the Co-Kriging method. *Environ. Geochem. Health* **2024**, *46*, 297. [CrossRef] [PubMed]
24. Khan, A.; Wang, X.; Gul, K.; Khuda, F.; Aly, Z.; Elseman, A.M. Microwave-assisted spent black tea leaves as cost-effective and powerful green adsorbent for the efficient removal of Eriochrome black T from aqueous solutions. *Egypt. J. Basic Appl. Sci.* **2018**, *5*, 171–182. [CrossRef]
25. Asztemborska, M.; Jakubiak, M.; Rykaczewska, M.; Bembenek, M.; Stęborowski, R.; Bystrzejewska-Piotrowska, G. Mycoextraction of radiolabeled cesium and strontium by Pleurotus eryngii mycelia in the presence of alumina nanoparticles: Sorption and accumulation studies. *J. Environ. Radioact.* **2016**, *164*, 190–196. [CrossRef] [PubMed]
26. Mulder, C.; Janssen, C.R. Application of Chernobyl caesium-137 fallout and naturally occurring lead-210 for standardization of time in moss samples: Recent pollen–flora relationships in the Allgäuer Alpen, Germany. *Rev. Palaeobot. Palynol.* **1998**, *103*, 23–40. [CrossRef]
27. Jellen, E.N.; Kolano, B.A.; Sederberg, M.C.; Bonifacio, A.; Maughan, P.J. Chenopodium. In *Wild Crop Relatives: Genomic and Breeding Resources: Legume Crops and Forages*; Kole, C., Ed.; Springer: Berlin/Heidelberg, Germany, 2011; pp. 35–61.
28. Hallstadius, L. A method for the electrodeposition of actinides. *Nucl. Instrum. Methods Phys. Res.* **1984**, *223*, 266–267. [CrossRef]
29. Exposito-Suarez, V.M.; Suarez-Navarro, J.A.; Aguado-Herreros, C.M.; Sanz, M.B.; Suarez-Navarro, M.J.; Caro, A. Increasing the recovery and selectivity of $^{238}$U, $^{235}$U, and $^{234}$U extraction with tri-n-butyl phosphate in mine tailing samples with a high copper content. *Anal. Chim. Acta* **2023**, *1259*, 341183. [CrossRef]
30. Suarez-Navarro, J.A.; Exposito-Suarez, V.M.; Crespo, M.T.; Sanchez-Castano, B.; Suarez-Navarro, M.J.; Gasco, C.; Barragan, M.; Gascon, J.L.; Pecker, R.; Sanchez-Perez, L.; et al. Improvements in the radiochemical method for separating $^{226}$Ra in solid samples through coprecipitation with $BaSO_4$. *Appl. Radiat. Isot.* **2022**, *187*, 110321. [CrossRef]
31. Cano, A.; Suarez-Navarro, J.A.; Puertas, F.; Fernandez-Jimenez, A.; Alonso, M.D.M. New Approach to Determine the Activity Concentration Index in Cements, Fly Ashes, and Slags on the Basis of Their Chemical Composition. *Materials* **2023**, *16*, 2677. [CrossRef]
32. Towett, E.K.; Shepherd, K.D.; Cadisch, G. Quantification of total element concentrations in soils using total X-ray fluorescence spectroscopy (TXRF). *Sci. Total Environ.* **2013**, *463–464*, 374–388. [CrossRef]
33. Heijerick, D.G.; Van Sprang, P.A.; Van Hyfte, A.D. Ambient copper concentrations in agricultural and natural European soils: An overview. *Environ. Toxicol. Chem.* **2006**, *25*, 858–864. [CrossRef]
34. Ballabio, C.; Panagos, P.; Lugato, E.; Huang, J.-H.; Orgiazzi, A.; Jones, A.; Fernández-Ugalde, O.; Borrelli, P.; Montanarella, L. Copper distribution in European topsoils: An assessment based on LUCAS soil survey. *Sci. Total Environ.* **2018**, *636*, 282–298. [CrossRef]
35. Badilla-Ohlbaum, R.; Ginocchio, R.; Rodríguez, P.H.; Céspedes, A.; González, S.; Allen, H.E.; Lagos, G.E. Relationship between soil copper content and copper content of selected crop plants in central Chile. *Environ. Toxicol. Chem.* **2001**, *20*, 2749–2757. [CrossRef] [PubMed]
36. Neiva, A.M.R.; Antunes, I.M.H.R.; Carvalho, P.C.S.; Santos, A.C.T. Uranium and arsenic contamination in the former Mondego Sul uranium mine area, Central Portugal. *J. Geochem. Explor.* **2016**, *162*, 1–15. [CrossRef]
37. Chmielewski, A.G.; Wawszczak, D.; Brykała, M. Possibility of uranium and rare metal recovery in the Polish copper mining industry. *Hydrometallurgy* **2016**, *159*, 12–18. [CrossRef]
38. Patra, A.C.; Sumesh, C.G.; Mohapatra, S.; Sahoo, S.K.; Tripathi, R.M.; Puranik, V.D. Long-term leaching of uranium from different waste matrices. *J. Environ. Manag.* **2011**, *92*, 919–925. [CrossRef]
39. Pehoiu, G.; Radulescu, C.; Muraresc u, O.; Dulama, I.D.; Bucurica, I.A.; Teodorescu, S.; Stirbescu, R.M. Health Risk Assessment Associated with Abandoned Copper and Uranium Mine Tailings. *Bull. Environ. Contam. Toxicol.* **2019**, *102*, 504–510. [CrossRef]
40. UNSCEAR. *Sources and Effects of Ionizing Radiation*; UNSCEAR 2000 Report to the General Assembly, with Scientific Annexes. Volume I: Sources; United Nations Scientific Committee on the Effects of Atomic Radiation: New York, NY, USA, 2000.
41. Suarez-Navarro, J.A.; Gil-Pacheco, E.; Exposito-Suarez, V.M.; Gomez-Mancebo, M.B.; Vicente-Prieto, N.; Garcia-Gomez, H.; Suarez-Navarro, M.J.; Sanchez-Gonzalez, S.M.; Caro, A.; Hernaiz, G.; et al. Influence of soil chemical composition on U, $^{226}$Ra and $^{210}$Pb uptake in leaves and fruits of *Quercus ilex* L. *J. Environ. Radioact.* **2023**, *264*, 107187. [CrossRef]
42. Gil-Pacheco, E.; Suarez-Navarro, J.A.; Sanchez-Gonzalez, S.M.; Suarez-Navarro, M.J.; Hernaiz, G.; Garcia-Sanchez, A. A radiological index for evaluating the impact of an abandoned uranium mining area in Salamanca, Western Spain. *Environ. Pollut.* **2020**, *258*, 113825. [CrossRef]
43. Hill, B.D. *Sequential Kaiser-Meyer-Olkin Procedure as an Alternative for Determining the Number of Factors in Common-Factor Analysis: A Monte Carlo Simulation*; Oklahoma State University: Stillwater, OK, USA, 2011.
44. Choi, S.-J.; Lee, B.-T.; Kim, J.-Y.; Kim, K.-W. Study on adsorption/desorption of As by mine sludge depending on pH and natural organic matter. *Geosystem Eng.* **2013**, *16*, 191–199. [CrossRef]

45. Lahrouch, F.; Guo, N.; Hunault, M.O.J.Y.; Solari, P.L.; Descostes, M.; Gerard, M. Uranium retention on iron oxyhydroxides in post-mining environmental conditions. *Chemosphere* **2021**, *264*, 128473. [CrossRef]
46. Stewart, B.D.; Cismasu, A.C.; Williams, K.H.; Peyton, B.M.; Nico, P.S. Reactivity of Uranium and Ferrous Iron with Natural Iron Oxyhydroxides. *Environ. Sci. Technol.* **2015**, *49*, 10357–10365. [CrossRef] [PubMed]
47. Liu, B.; Peng, T.; Sun, H.; Yue, H. Release behavior of uranium in uranium mill tailings under environmental conditions. *J. Environ. Radioact.* **2017**, *171*, 160–168. [CrossRef] [PubMed]
48. Expósito-Suárez, V.M.; Suárez-Navarro, J.A.; Caro, A.; Sanz, M.B.; Gómez-Mancebo, M.B.; Barragán, M.; Suárez-Navarro, M.J.; Ferreiro, A.; Fitzgerald, T.; Sánchez-Sánchez, P.; et al. Model of U and $^{226}$Ra uptake by Spergularia rubra (L.) J. Presl & C. Presl in an area affected by Cu ore mining. *J. Radioanal. Nucl. Chem.* **2024**, 1–15. [CrossRef]
49. Moldovan, B.J.; Jiang, D.T.; Hendry, M.J. Mineralogical Characterization of Arsenic in Uranium Mine Tailings Precipitated from Iron-Rich Hydrometallurgical Solutions. *Environ. Sci. Technol.* **2003**, *37*, 873–879. [CrossRef]
50. Al-Masri, M.S.; Arabi, M.I.E.; Al-Daoude, A.; Khalily, H.; Amin, Y.; Shoaib, A.; Al-Khateeb, Y.; Al-Masri, W.; Khalill, I.; Aboud, O. Comparison of transfers for natural radionuclides ($^{238}$U, $^{234}$Th, $^{226}$Ra, $^{210}$Pb & $^{210}$Po) from five different soils to four different barley genotypes. *J. Radioanal. Nucl. Chem.* **2022**, *331*, 3439–3447. [CrossRef]
51. Ross, E.M.; Raj, Y.L.; Wesley, S.G.; Rajan, M.P. Selected natural and fallout radionuclides in plant foods around the Kudankulam Nuclear Power Project, India. *J. Environ. Radioact.* **2013**, *115*, 201–206. [CrossRef]
52. Linsalata, P. Uranium and thorium decay series radionuclides in human and animal foodchains—A review. *J. Environ. Qual.* **1994**, *23*, 633–642. [CrossRef]
53. Vandenhove, H.; Van Hees, M. Phytoextraction for clean-up of low-level uranium contaminated soil evaluated. *J. Environ. Radioact.* **2004**, *72*, 41–45. [CrossRef]
54. Blanco Rodríguez, P.; Vera Tomé, F.; Lozano, J.C.; Pérez Fernández, M.A. Transfer of $^{238}$U, $^{230}$Th, $^{226}$Ra, and $^{210}$Pb from soils to tree and shrub species in a Mediterranean area. *Appl. Radiat. Isot.* **2010**, *68*, 1154–1159. [CrossRef]
55. El-Mesbahi, M.N.; Azcón, R.; Ruiz-Lozano, J.M.; Aroca, R. Plant potassium content modifies the effects of arbuscular mycorrhizal symbiosis on root hydraulic properties in maize plants. *Mycorrhiza* **2012**, *22*, 555–564. [CrossRef]
56. Gil-Pacheco, E.; Suárez-Navarro, J.A.; Fernández-Salegui, A.B.; Sánchez-González, S.M.; Suarez-Navarro, M.J.; García-Sánchez, A. Factors that influence the absorption of uranium by indigenous plants on the spoil tip of an abandoned mine in western Spain. *Sci. Total Environ.* **2021**, *759*, 143571. [CrossRef] [PubMed]
57. Nakanishi, T.M. Research with radiation and radioisotopes to better understand plant physiology and agricultural consequences of radioactive contamination from the Fukushima Daiichi nuclear accident. *J. Radioanal. Nucl. Chem.* **2017**, *311*, 947–971. [CrossRef]
58. Rubinos, D.A.; Barral, M.T. Fractionation and mobility of metals in bauxite red mud. *Environ. Sci. Pollut. Res.* **2013**, *20*, 7787–7802. [CrossRef]
59. Suárez-Navarro, J.A.; Alonso, M.M.; Gascó, C.; Pachón, A.; Carmona-Quiroga, P.M.; Argiz, C.; Sanjuán, M.Á.; Puertas, F. Effect of particle size and composition of granitic sands on the radiological behaviour of mortars. *Bol. Soc. Esp. Cerám. Vidr.* **2021**, *61*, 561–573. [CrossRef]
60. Bachmaf, S.; Merkel, B.J. Sorption of uranium(VI) at the clay mineral–water interface. *Environ. Earth Sci.* **2011**, *63*, 925–934. [CrossRef]
61. Yamaguchi, A.; Kurihara, Y.; Nagata, K.; Tanaka, K.; Higaki, S.; Kobayashi, T.; Tanida, H.; Ohara, Y.; Yokoyama, K.; Yaita, T.; et al. Molecular geochemistry of radium: A key to understanding cation adsorption reaction on clay minerals. *J. Colloid Interface Sci.* **2024**, *661*, 317–332. [CrossRef]
62. Greeman, D.J.; Rose, A.W.; Washington, J.W.; Dobos, R.R.; Ciolkosz, E.J. Geochemistry of radium in soils of the Eastern United States. *Appl. Geochem.* **1999**, *14*, 365–385. [CrossRef]
63. Rufyikiri, G.; Huysmans, L.; Wannijn, J.; Van Hees, M.; Leyval, C.; Jakobsen, I. Arbuscular mycorrhizal fungi can decrease the uptake of uranium by subterranean clover grown at high levels of uranium in soil. *Environ. Pollut.* **2004**, *130*, 427–436. [CrossRef]
64. Chen, B.; Zhu, Y.-G.; Zhang, X.; Jakobsen, I. The influence of mycorrhiza on uranium and phosphorus uptake by barley plants from a field-contaminated soil (7 pp). *Environ. Sci. Pollut. Res.* **2005**, *12*, 325–331. [CrossRef]
65. Rufyikiri, G.; Thiry, Y.; Declerck, S. Contribution of hyphae and roots to uranium uptake and translocation by arbuscular mycorrhizal carrot roots under root-organ culture conditions. *N. Phytol.* **2003**, *158*, 391–399. [CrossRef]